Defence Science Journal, Vol. 70, No. 5, September 2020, pp. 564-570, DOI : 10.14429/dsj.70.15228


# Analysis of Operating Principles and Flow Field Characteristics for a Diving Ballast Tank

K.C. Pan* and I.M. Chao

*Department of Power Vehicle and Systems Engineering, Chung Cheng Institute of Technology, National Defense University, Taoyuan, Taiwan, ROC*
**E-mail: pankc@url.com.tw*

**ABSTRACT**

Operating principle and flow field characteristics of a diving ballast tank for application in submerged vehicles were investigated in the present study. As understanding the complex changes in the interior air-water two-phase flow field of the ballast tank during the diving process is difficult, this study specifically performed a ballast tank diving experiment. Experimental and numerical simulations to analyse the diving motions of the ballast tank were conducted. Authors comprehensively evaluated the flow field changes in the ballast tank and its surroundings. The experimental and numerical results were compared in terms of the observed displacements and velocities during diving. Both the results indicated similar motion trajectories and velocities. Authors effectively observed the air-water two-phase flow field change inside the ballast tank using this numerical method. Therefore, the numerical model constructed in this study can be useful for analysing the diving motions of ballast tanks and can effectively predict the interior flow field characteristics of a ballast tank.

**Keywords:** Ballast tank; Submerged vehicle; Computational fluid dynamics; Dynamic mesh model

## 1. INTRODUCTION

Exploring oceans is mysterious and challenging. Throughout human history, numerous records exist on the construction of submerged vehicles to carry personnel to perform underwater tests, for application in fields such as scientific research, resource exploration, or military purposes. However, regardless of the type of submerged vehicles, in addition to the overall design of submerged vehicles and a complete personnel maintenance system, navigation stability and motion attitude control of submerged vehicles must be understood. This understanding is critical for operators to work in uncertain and high-risk waters; to this end, the configuration and operation of the ballast tank are undoubtedly key aspects in the design of a submerged vehicle.

The diving and floating process constitutes an extremely important part of a moving submerged vehicle. When a vehicle floats on water, the buoyancy of water is equal to its weight. Therefore, water must be introduced into the ballast tank to increase the weight of the vehicle to enable diving operations[1]. During the diving process, the centre of gravity and centre of buoyancy, which are special for moving submerged vehicles, will change as water enters the tank[2]. Controlling the diving and floating mechanisms by adjusting the water level in the ballast tank appears easy; however, in practice, many parameters are yet to be determined through professional designing, wherein experiments are required to verify the effectiveness. Typically, a vehicle to be submerged must have fast diving abilities, and more importantly, it should submerge in a stable and silent manner[3,4]. Therefore, the water level in the ballast tank must be precisely controlled to balance buoyancy and weight[5].

In this study, experimental observations and numerical simulation results were used to analyse the flow field in a diving ballast tank. As the movement of submerged vehicles is closely related to the operation of the ballast tank, relevant prior literature was first surveyed[6]. Font and García-Peláez[7] analysed the influence of water levels in the ballast tank on the movement of submarines. They suggested that under different submerged depths, high accuracy and quick responses could be achieved through water level adjustments. Woods[8], *et al.* found that submerged depths could be controlled by adjusting the level of the ballast tank, where propeller operations could be reduced at low speeds. Liu[9] employed a mathematical model for submarine motion to develop a submarine handling simulation system. A mathematical model of the ballast tank operation was introduced to investigate the influence of ballast tank operations on the mathematical model of submarine motion. Tiwari and Sharma[10] used a simulation model for studying flexible buoyancy systems (FBSs) in underwater vehicles (UVs). Their results proved the applicability of FBSs for UVs from low to high ranges of operating depths. Sinaga[11] experimented with a mini submarine to analyse the pitching motion when transitioning from snorkelling to diving. The change in the position of the vertical centre of gravity significantly affected the angle of attack of the mini submarine.

Further, in the flow field simulation of the ballast tank, this study used the dynamic mesh model (DMM) to simulate the diving motion of the ballast tank. Previously, Lei[12] employed the DMM to simulate the flow field in underwater body motions to

Received : 23 October 2019, Revised : 10 June 2020
Accepted : 31 July 2020, Online published : 08 October 2020

explore the changes in the surrounding flow field and pressure distribution due to different submerged body movements. Guo[13] used the DMM to analyse the spectral characteristics of water surface disturbance caused by a snorkelling submarine and further investigate the influence of submarine motion on the wave spectrum under different submarine depths and speeds. Lin[14] employed the laying mesh technique, which is capable of handling dynamic meshes, to simulate a floating submarine and calculate its motion resistance. Furthermore, Yang[15] used the computational fluid dynamics to simulate changes in the surrounding flow field of a submarine under oblique cruising conditions and investigate the pressure distribution of the submarine under different underwater motion attitudes. Ahmadzadeh[16], *et al.* investigated the relationship between the changes in the underwater velocity of spheres and underwater resistance against spheres, where the spheres had different densities and were vertically dropped into water at the same velocity. Pan[17] employed the DMM to simulate a torpedo moving into water, where the influence of gravity and buoyancy on the acceleration changes in the submerged torpedo was calculated. Dubbioso[18] simulated a submarine sailing both at infinite depth and near the free surface (snorkelling operation) to analysed the impact of the cross rudder and X rudder on the operating performance of the submarine. The diving motion, affected by gravity and buoyancy, is closely related to the design of the ballast tank of the submerged vehicle.

The ballast tank is the main component of a submerged vehicle. The movements of submerged vehicles rely on the stable and efficient operation of the ballast tank. Even during vehicle navigation, posture adjustments must be performed by adjusting the intake and drainage of the ballast tank. Thus, efficient operation of the ballast tank is very important for navigating submerged vehicles; therefore, when initially exploring the movement of the ballast tank, this study first analysed the diving motion of the ballast tank. It helped observe and analyse the complex two-phase flow field inside the ballast tank.

In summary, this study first conducted a diving motion experiment with a ballast tank to investigate the flow field characteristics in ballast tank operations, based on which simulations of three-dimensional flow fields around the diving ballast tank were performed. Finally, the numerical results were compared with their experimental counterparts to verify that the numerical model constructed in this study could effectively analyse flow fields during ballast tank motion. The numerical model developed in this study can be used as a reference when designing ballast tanks for underwater vehicles.

## 2. EXPERIMENT FOR ANALYSING DIVING MOTION OF THE BALLAST TANK

For performing the experiment to study the diving motion of a ballast tank, transparent acrylic plates were used to construct a cubic ballast tank model to easily observe its motions. The model had a side length of 20 cm and wall thickness of 1 cm, with its interior being able to accommodate the inflow of water. Two holes having identical areas of $4\pi$ cm$^2$ were drilled to form a passage; one hole was at the top of the ballast tank, and the other one was at the bottom. However, owing to limitations in terms of the existing experimental equipment and funding, constructing a large ballast tank was beyond our capacity. Therefore, a small tank measuring 180 cm × 90 cm × 90 cm was constructed for the experiment, as shown in Fig. 1. In addition, for investigating the flow fields in the diving motion of the ballast tank, the six-degree-of-freedom movement was temporarily neglected. Therefore, experiments considering diving motions along a single direction were performed. To this end, the ballast tank model was supported using buckles and cables to enable its movement in the vertical direction, as shown in Fig. 2.

In addition, owing to the experimental environment and funding constraints, we could not use very precise experimental equipment; therefore, the experiment simply explored the displacement and velocity of the diving ballast tank. The experiment observed the process of diving ballast tank with a camera and measured the displacement based on the scale outside the ballast tank and water level scale inside the water tank. In this study, the camera took a screenshot every 0.03 s. The diving process of the ballast tank was 1.63s, the confidence limits were 1.63±0.015 s, and the relative uncertainty is 0.92%. Besides, the total displacement of the diving motion of the ballast tank was 0.3 m, the least count of the scale was 0.001 m, and the relative uncertainty is 0.17 %. Therefore, the relative uncertainty of the results is 0.94% on the 95 percent confidence level by analysing the propagation of uncertainty in calculations.

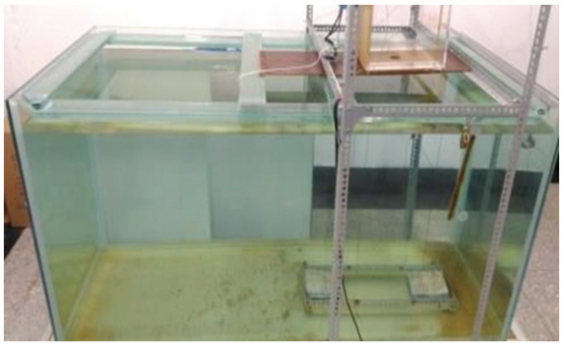

**Figure 1. Experimental setup for studying diving motion of the ballast tank.**

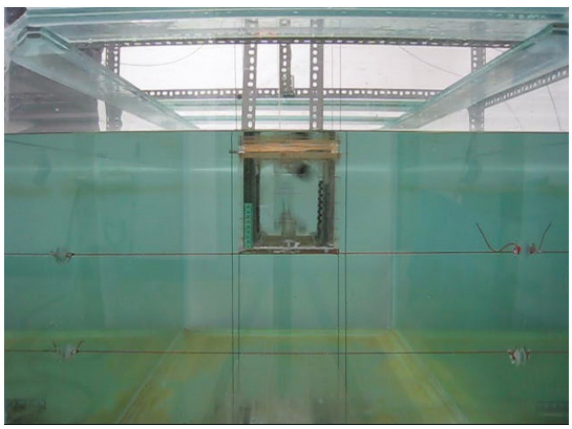

**Figure 2. Schematic showing diving motion of the ballast tank.**

## 3. NUMERICAL SIMULATION METHODS

### 3.1 Governing Equations

This study aimed to investigate the flow field characteristics during ballast tank motion. In the diving process of the ballast tank, changes in the air-water two-phase flow field incurred in the interior of the tank. Therefore, when simulating the ballast tank motion, the Reynolds-Averaged Navier-Stokes (RANS) equations, considering the fluid viscosity effect, were used as the governing equations. The RANS equations include continuity and momentum equations, and can be expressed as follows in the Cartesian tensor form[19]:

$$\frac{\partial \rho}{\partial t}+\frac{\partial}{\partial x_i}(\rho u_i)=0 \tag{1}$$

$$\frac{\partial}{\partial t}(\rho u_i)+\frac{\partial}{\partial x_j}(\rho u_i u_j)=-\frac{\partial p}{\partial x_i}+\frac{\partial}{\partial x_j}\left[\mu\left(\frac{\partial u_i}{\partial x_j}+\frac{\partial u_j}{\partial x_i}-\frac{2}{3}\delta_{ij}\frac{\partial u_l}{\partial x_l}\right)\right]+\frac{\partial}{\partial x_j}\left(-\rho\overline{u_i' u_j'}\right) \tag{2}$$

In these equations, $u_i$ is the average velocity, $p$ is the pressure, $\delta_{ij}$ represents the Kronecker delta and $\overline{u_i' u_j'}$ represents Reynolds Stress. It is the derivative of the time-averaged Navier-Stokes equations, causing simultaneous Eqns. (1) and (2) to become unclosed. Therefore, this study used the $k$-ω turbulence model to replace Eqns. (1) and (2). Thus, the number of unknowns in the RANS equations became equal to the number of equations, indicating that the equations could be solved easily. In the numerical simulations, we used ANSYS® Fluent® version 18.0, a software package based on the finite volume method (FVM) to solve the flow field. The FVM, currently a mature discrete numerical model, is capable of improving the accuracy of flow field calculations as well as the efficiency of equation solving (Parameter settings are given in Table 1).

**Table 1. Parameter settings of turbulence model**

| | | | |
|---|---|---|---|
| Model | Solver | Formulation | Absolute |
| | | Time | Transient |
| | Viscous Model | | SST $k$–$\omega$ |
| | Pressure–Velocity Coupling | | Coupled |
| Solution | Discretisation | Pressure | PRESTO! |
| | | Momentum | Second Order Upwind |
| | | Turbulence Kinetic Energy | Second Order Upwind |
| | | Turbulence Dissipation Rate | First Order Upwind |

### 3.2 Volume of Fluid

Because the diving of the ballast tank involves flow field motions in the air and water phases, the resulting free surface distribution has a significant influence on the form resistance and friction resistance against the ballast tank. Therefore, the free surface effect and two-phase flow field had to be considered numerically. To address this issue, we employed the volume of fluid (VOF) scheme which was originally developed by Hirt and Nichols[20] to solve the free surface motion problem. In the VOF scheme, the flow field calculation domain was divided into many small mesh blocks; a two-phase flow function was defined for each mesh block, with the function value between 0 and 1. The equation for determining the position of the free surface can be expressed as follows[21]:

$$\frac{\partial a_q}{\partial t}+\vec{u}_i\cdot\nabla a_q=0 \tag{3}$$

where $\alpha_q$ represents the volume of the water; $\alpha_q = 0$ indicates that the fluid medium is air; $\alpha_q = 1$ indicates that the fluid medium is water. When $0 < \alpha_q < 1$, the media of the fluid is considered a coexistence of air and water, and $\alpha_q = 0.5$ reflects the position of the free surface. In this study, when applying VOF scheme to solve the free surface problem, the free surface condition of the flow field in the calculation domain was first defined as $\alpha_q = 0.5$. By linking each small block of the two-phase flow function, the VOF scheme captured the states of free surface changes in the flow field.

### 3.3 Dynamic Mesh Model

During the diving motion simulations of the ballast tank, the flow field meshes around the ballast tank usually required adjustments based on the displacement of the ballast tank. Otherwise, the quality of the surrounding mesh would deteriorate owing to the movement of the ballast tank; negative volume meshes could be generated, causing the calculation to terminate. Therefore, this study employed the DMM to address the calculation problems regarding flow field meshes associated with the ballast tank motion. The DMM can effectively address the grid configuration problem created after the movement of objects, wherein an independent block of meshes encircle the simulation object to be moved. As this independent mesh block moved in the computational domain, the grid points around its surface changed as the object moved; the meshes around the moving path compressed or stretched, causing the meshes to regenerate, thus avoiding mesh overlap. In general, the DMM is suitable for dynamic simulation of objects with arbitrary motion trajectories and offers high flexibility in mesh configurations.

## 4. MESH CONSTRUCTION AND BOUNDARY CONDITION SETTINGS FOR THE COMPUTATIONAL DOMAIN OF FLOW FIELDS

For simulating the diving motion of a ballast tank, Rhinoceros CAD software was used to design a 20-cm-long cubic ballast tank with 1-cm-thick walls. The tank interior was allowed to accommodate the inflow of water; the opening area at the bottom of the ballast tank was set to $4\pi$ cm$^2$, identical to that used in the previous experiment. The flow field domain was 90 cm long, 90 cm wide, and 110 cm high, as shown in Fig. 3. In computational domain grid layout used for the simulation, an independent block of meshes was employed to encircle the tank; structured meshes were generated inside the ballast tank and in the vicinity of the exterior surface to ensure grid quality and calculation accuracy of the flow field.

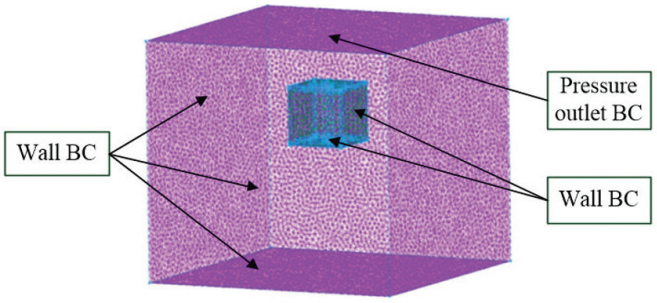


**Figure 3. Schematic showing the boundary condition used simulating for the diving motion of the ballast tank.**

The mesh numbers contained in the computational domain are 683,562. Further, in the region outside the independent block, the DMM was applied with unstructured meshes. The non-slip boundary condition (BC) was imposed on the internal and external surfaces of the tank, and bottom of the computational domain and its surrounding surfaces, and the pressure outlet BC was imposed on the top of the computational domain.

Furthermore, a user-defined function was used to enable vertical motion of the tank, wherein the weight of the ballast tank was set to balance the buoyancy force. Initially, the top of the ballast tank was assumed to overlap with part of the free surface. At this instance, the tank was completely submerged in water. In case of an empty tank, the movement position of the ballast tank in the next time step was calculated considering the relationship between the gravity and buoyancy in the flow fields.

## 5. RESULTS AND DISCUSSION

To explore the influence of the numerical result by using different mesh numbers, this paper had employed simulation examples that include different mesh numbers. The mesh numbers contained in mesh type A and B are 683,562 and 962,361, respectively. As shown in Fig. 4, with increasing of the mesh numbers, the numerical results are getting more and more close to the experimental data. The result shows that mesh numbers deeply affected the numerical results. However, more sophisticated computers are required to perform more accurate numerical simulations, and it is also based on the computers used in this study cannot smoothly and fully execute such a large number of mesh calculations. The authors conducted detailed numerical simulations with mesh type A, and the numerical calculation results will be used for subsequent exploration and analysis.

Figure 5 shows the flow field changes observed during the diving motion simulation of the ballast tank, where blue represents air, red represents water, and the remaining portion represents the coexistence of air and water. The tank moved downward after being releasing from the free surface, causing the water flowing into the tank to be injected upward like a water column, with a tendency of gradually spreading. Moreover, Fig. 5 clearly shows the flow field changes in the two-phase air-water flow. It also shows the changes in the flow field occurring when air was compressed from the inside of the tank to the free surface. All of the above phenomena are

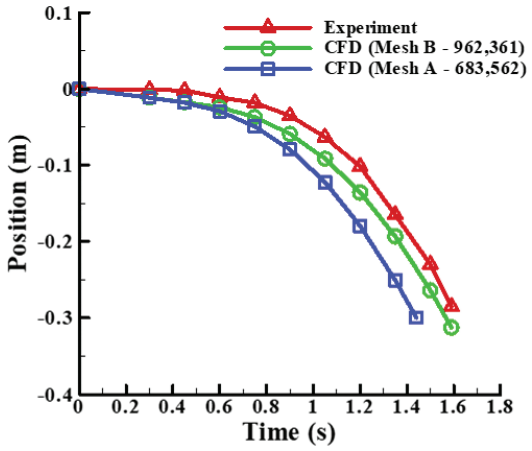


**Figure 4. Grid dependency study for diving motion of the ballast tank.**

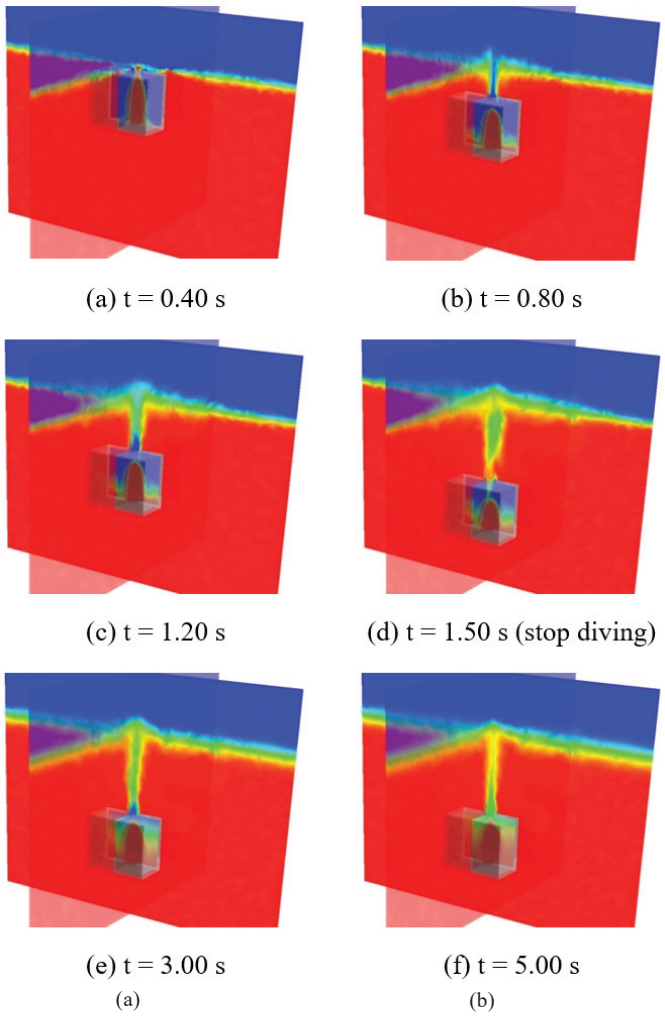


**Figure 5. Variations in the flow fields at different simulation times during diving motions of the ballast tank. (a) t = 0.40 s, (b) t = 0.80 s, (c) t = 1.20 s, (d) t = 1.50 s (stop diving), (e) t = 3.00 s, and (f) t = 5.00 s.**

indispensable and constitute important flow field information used in the design of ballast tanks for submerged vehicles. Although the variations in the flow fields during diving motions of the ballast tank were similar and coherent with the

physical characteristics of motion flow fields expected for the ballast tank, numerical analysis was conducted because this study exclusively focused on developing practical numerical calculation models for analysing the diving motions of ballast tanks.

Figure 6 compares the flow field variations observed experimentally and in the numerical simulations for evaluating the diving motions of the ballast tank. High similarity is observed in the free surface changes of the tank interior between the two results. First, during the experiment, a violent water jet was generated inside the ballast tank, and an air-water two-phase flow field was formed. Furthermore, changes in the simulated flow field indicate water column injection inside the water tank. Here, the part in green around the water column indicates the coexistence of water and air, which is similar to the experimentally observed flow field inside the tank. In addition, Fig. 6 clearly shows that the ballast tank stopped after reaching the set depth. At this instance, the height of the water column inside the ballast tank also decreased along with the sudden decrease in speed; this height then increased because of the influence of water pressure, which was confirmed by observing the water-air two-phase flow field changes inside the ballast tank.

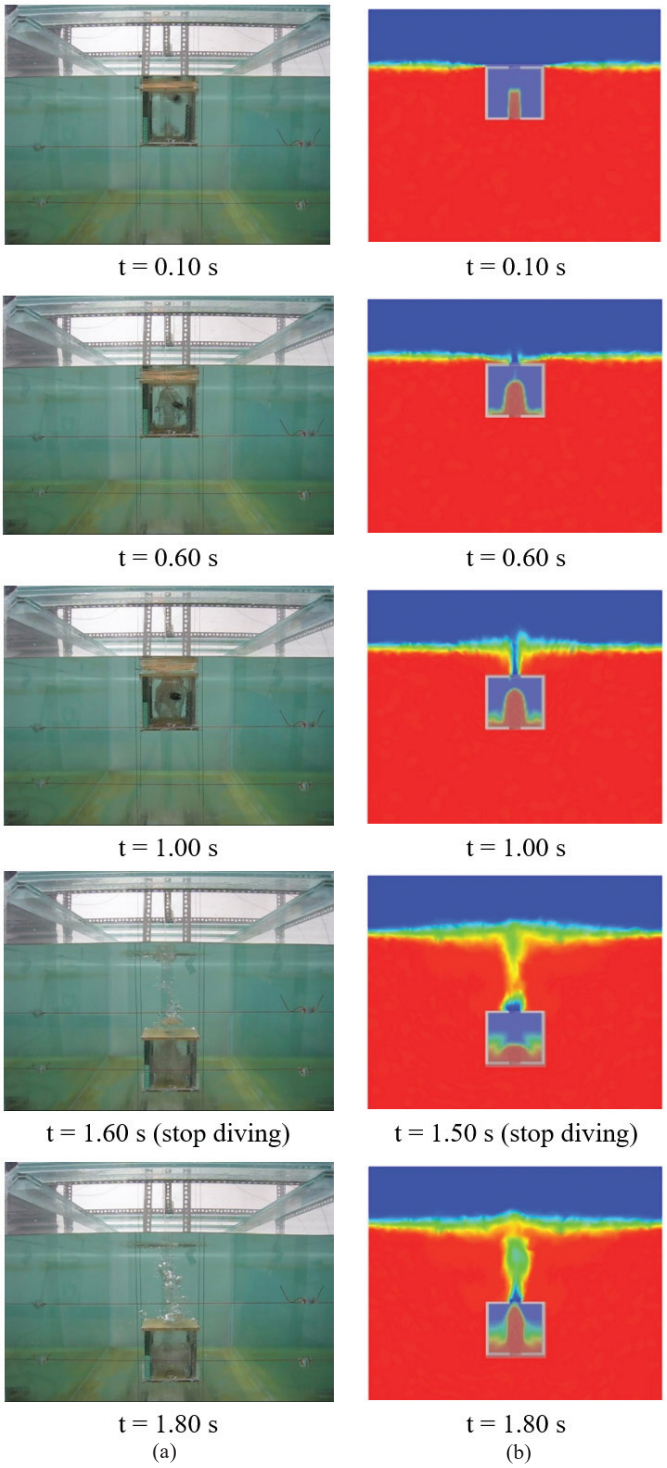


**Figure 6. Diving motions of the ballast tank at different times. (a) experimental and (b) numerical simulation.**

Figure 7 shows the displacement changes with time in the experimental and numerical results for the diving motion of the ballast tank. During the experiment, the ballast tank was nearly stagnant before t = 0.4 s; conversely, in the numerical simulation, although the ballast tank moved downward before t = 0.4 s, there was only a slight displacement. However, the displacement of the ballast tank gradually increased rapidly after t = 0.4 s during the numerical simulation, whereas it increased slowly at after = 0.4 s during the experiment. This can be attributed to the fact that the buckles and cables around the ballast tank exterior generated friction during motion, which affected the diving motion of the ballast tank in the experiment; however, the displacement of the physical ballast tank also gradually increased. Finally, although there are differences between the experimental and numerical calculation results, their trajectories show the same development trend.

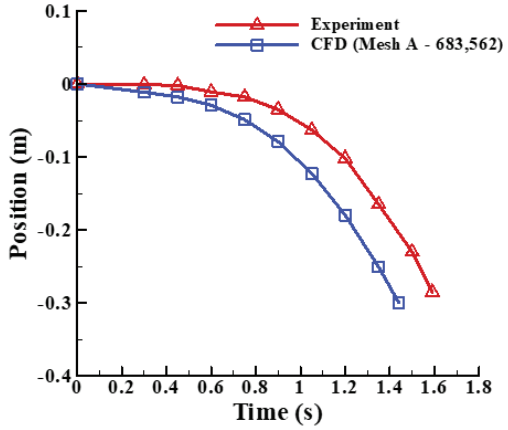


**Figure 7. Variations in displacement at different simulation times during diving motion of the ballast tank.**

Figure 8 exhibits the velocity variations at different time intervals observed in the experiment and numerical simulation. In the initial stage during the numerical simulation, the diving velocity of the ballast tank slowly increased and then gradually decreased. This suggests that micro oscillations were generated inside the tank during its motion. At t = 0.4s, the diving velocity of the ballast tank began continuously increasing. This situation can be compared to the diving motions of the ballast tank in Fig. 6, during the initial stage of the experiment and numerical simulation, water was injected into the tank in the form of a jet. During this period, when water entered the tank and had not

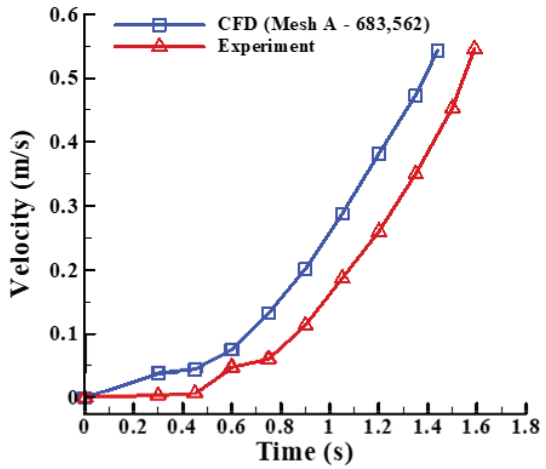


**Figure 8. Variations in velocity at different simulation times during diving motion of the ballast tank.**

reached the tank bottom, the weight of the jet had not exerted its influence. Therefore, the tank diving velocity had not increased. However, after the water column spread to the tank bottom, the diving velocity began to continuously increase. Figure 8 also shows that at the initial stage of the experiment, the tank did not dive at a high velocity, which was possibly because of the friction generated by the cables. Moreover, after t = 0.4 s, the diving velocity of the tank suddenly increased, conforming to the results shown in Fig. 7. Finally, Fig. 8 shows that the velocity of the diving ballast tank is still increasing, so it reveals that the motion of the ballast tank has not approached the terminal velocity. With regard to the results, the influence of gravity and buoyancy on the acceleration changes in the diving ballast tank will be an important topic for future research.

In summary, although the experimental and numerical results presented in Figs. 7 and 8 are slightly different, their overall displacement and velocity variations show a high degree of similarity. Furthermore, the numerical model established in this study can be to investigate and analyse ballast tank diving motions. It can provide researchers with an effective numerical calculation method in the future.

## 6. CONCLUSION

This study aimed to investigate the flow field characteristics of a diving ballast tank through experiments and numerical simulations. According to the research results, the numerical calculation model developed for analysing the diving motion of the ballast tank can effectively observe the air-water two-phase flow field change inside the ballast tank. In addition, the numerical simulation and experimental results help understand the operation characteristics of the ballast tank. Besides, comparisons between numerical and experimental results indicated similar motion trajectories and velocities; moreover, we observed similarities in the flow field variations inside the ballast tank. These findings suggest that the numerical method used in this study could be used to effectively analyse the motion flow fields of ballast tanks. These results provide important flow field information useful to explore the operations of ballast tanks and can be used as a reference for designing ballast tanks.

The numerical calculation model established in this study provided preliminary results regarding the diving motion simulation of a ballast tank. Furthermore, it can be used as an effective analysis method for different diving motions of ballast tanks. In future, if it can be combined with numerical calculation models for evaluating the floating motions of ballast tanks, it can comprehensively analyse the flow field characteristics during diving and floating motions of ballast tanks, and expecting to be practically applied in designing ballast tanks for submerged vehicles.

## REFERENCES

1. Renilson, M. Submarine hydrodynamics. Springer, USA, 2015, pp. 5-17.
2. Burcher, R. & Rydill, L. Concepts in submarine design. Cambridge University Press, UK, 1994, pp. 52-70. doi: 10.1017/CB09781107050211
3. Kedarnath Shenoy, S. & Sanilkumar, K.V. Anti-submarine warfare oceanography. *Def. Sci. J.*, 2019, **69**(2), 107-108. doi: 10.14429/dsj.69.14216
4. Moh,T.; Jang, N.; Jang, S. & Cho, J.H. Application of a winch-type towed acoustic sensor to a wave-powered unmanned surface vehicle. *Def. Sci. J.*, 2017, **67**(1), 125-128. doi: 10.14429/dsj.67.10577
5. Meyerhofer, P. & Hartwig, J. Trade study of advanced ballast control systems for an extraterrestrial submarine. *Ocean Eng.*, 2019, **171**, 1-13. doi: 10.1016/j.oceaneng.2018.10.055
6. Tusar, M.H.; Hasan, Md.K.; Sikder, M.A.B.; Chowdhury, N.B. & Fakir, M.H. Design and fabrication of a low cost ballast system for distant controlled submarine. *In* Proceedings of the International Conference on Mechanical Engineering and Renewable Energy (ICMERE2015-PI-269), Chittagong, Bangladesh, 2015.
7. Font, R. & García-Peláez, J. On a submarine hovering system based on blowing and venting of ballast tanks. *Ocean Eng.*, 2013, **72**, 441-447. doi: 10.1016/j.oceaneng.2013.07.021
8. Woods, S.A.; Bauer, R.J. & Seto, M.L. Automated ballast tank control system for autonomous underwater vehicles. *IEEE J. Oceanic Eng.*, 2012, **37**, 727-739. doi: 10.1109/JOE.2012.2205313
9. Liu, W.C. Development for a simulation system of submarine maneuvering motions by applying modular mathematical model. National Taiwan University, Taiwan ROC, 2015. (Master Thesis)
10. Tiwari, B.K. & Sharma, R. A computing model for design of flexible buoyancy system for autonomous underwater vehicles and gliders. *Def. Sci. J.*, 2018, **68**(6), 589-596. doi: 10.14429/dsj.68.12548
11. Sinaga, L.T.P. Experimental analysis of pitching motion in various angle of attack for mini submarine on surface condition. *Int. J. Mech. Eng. Rob. Res.*, 2018, **7**(1), 46-50. doi: 10.18178/ijmerr.7.1.46-50
12. Lei, C.Y. Research of develop the unstructured moving mesh technique to predict the hydrodynamic performance

of such underwater military vehicle. National Defense University, Taiwan ROC, 2005. (Master Thesis)
13. Guo, Z.M. Investigation of wave spectrum characteristics of moving underwater submarines. National Defense University, Taiwan ROC, 2008. (Master Thesis)
14. Lin, H.H. Numerical flow simulation and resistance analysis for submarines under vertical rising motion. National Defense University, Taiwan ROC, 2013. (Master Thesis)
15. Yang, M.W. Computation of turbulent flow around submarine under oblique towing condition. National Taiwan University, Taiwan ROC, 2005. (Master Thesis)
16. Ahmadzadeh, M.; Saranjam, B.; Hoseini Fard, A. & Binesh, A.R. Numerical simulation of sphere water entry problem using Eulerian-Lagrangian method. *Appl. Math. Model.*, 2014, **38**, 1673-1684. doi: 10.1016/j.apm.2013.09.005
17. Pan, K.C. The computation of hydrodynamic force exerting on a navel mine dropping into water. National Defense University, Taiwan ROC, 2014. (Master Thesis)
18. Dubbioso, G.; Broglia, R. & Zaghi, S. CFD analysis of turning abilities of a submarine model. *Ocean Eng.*, 2017, **129**, 459–479. doi: 10.1016/j.oceaneng.2016.10.046
19. ANSYS, Inc. ANSYS Fluent Theory Guide. ANSYS, Inc., Southpointe, 2017.
20. Hirt, C.W. & Nichols, B.D. Volume of fluid (VOF) method for the dynamics of free boundaries. *J. Comput. Phys*., 1981, **39**, 201-225. doi: 10.1016/0021-9991(81)90145-5
21. Jang, J.Y.; Liu, T.L.; Pan, K.C.; & Chu, T.W. Numerical investigation on the hydrodynamic performance of amphibious wheeled armored vehicles. *J. Chin. Inst. Eng*., 2019, **42**, 700-711. doi: 10.1080/02533839.2019.1660225

## CONTRIBUTORS

**Dr K.C. Pan** is an Assistant Professor at the Department of Power Vehicle and Systems Engineering, Chung Cheng Institute of Technology, National Defense University, Taoyuan, Taiwan, ROC. His major research interests include : Computational fluid dynamics applications, naval architecture, and ocean engineering. He is involved in teaching and research in the fields of shipbuilding and ocean engineering.
In the current study, he provided overall guidance and supervision, and edited the paper.

**Mr I.M. Chao** obtained his master's from Department of Power Vehicle and Systems Engineering, Chung Cheng Institute of Technology, National Defense University, Taoyuan, Taiwan, ROC. His research areas include : Computational fluid dynamics applications.
In the current study, he performed the experiments and numerical simulations, and data analysis.